Inversion of Kinetic and Thermodynamic Preferences in Meisenheimer Complex formation: Regioselectivity in the Reaction of 2,4,6-Trimethylphenoxide Ion with 2,4,6-Trinitroanisole and the Importance of Stereoelectronic Factors

Richard A. Manderville and Erwin Buncel*

Contribution from the Department of Chemistry, Queen's University, Kingston, Ontario, Canada, K7L 3N6

Received April 6, 1993®

Abstract: To probe regioselectivity in Meisenheimer complexation, the reaction of 2,4,6-trimethylphenoxide ion ($MesO^-$) with 2,4,6-trinitroanisole (TNA) was followed by ^1H and ^{13}C NMR spectroscopy in the new low-temperature solvent acetonitrile–glyme (1:1, v/v) at –40 °C to ambient temperatures. The key results include finding a kinetic preference for C-1 attachment and that the σ-adduct that results from C-3 attack is thermodynamically more stable (K1T3 behavior); this behavior is in direct contrast to the "normal" C-3 to C-1 isomerization pathway displayed by alkoxides and hydroxide with TNA (K3T1 behavior) as well as different from the regioselectivity shown by the phenoxide ion as an O-nucleophile (K1T1 behavior). Stereoelectronic stabilization of C-1 O-adducts through n–σ* interaction of antiperiplanar lone pairs with the requisite C–O acceptor bonds is recognized as a major factor in the regioselectivity of C-1 versus that of C-3 attack. Such an antiperiplanar conformer is found to be energetically inaccessible for the C-1 TNA·$OMes^-$ adduct **3**, unlike the C-1 TNA·OMe^- adduct **4**. Estimation of the kinetic barriers and thermodynamics of adduct formation demonstrates the instability of **3** relative to that of **4** and thereby provides a basis for the slide or metamorphosis of K3T1 to K1T3 behavior.

Introduction

Studies of the reactions of nucleophiles, especially alkoxides, with picryl ethers, such as 2,4,6-trinitroanisole (TNA, **1**) and related substrates,[1] have been of wide interest.[2] In these systems, formation of a kinetically-preferred, C-3 anionic σ-bonded (Meisenheimer) adduct that isomerizes to a more stable C-1 adduct (now classified as K3T1 behavior; kinetic preference for C-3 and thermodynamic preference for C-1) is the usual pattern of regioselectivity and has been taken to be ubiquitous.[1,2] However, recently[3] we have challenged this view by showing, through the use of low-temperature ^1H NMR spectroscopy, that the reaction of **1** with the ambident (O- and C-) aryloxide nucleophile, the phenoxide ion, yields the C-1 adduct **2** as the first and only detectable phenoxide O-adduct at –40 °C in acetonitrile–glyme (CD_3CN-glyme-d_{10} 1:1, v/v). No evidence for formation of the C-3 phenoxide O-adduct **6** was found, and thus, the TNA/PhO^- system was classified as showing K1T1 (kinetic and thermodynamic preference for C-1) behavior for PhO^- acting as an O-nucleophile. In accord with the ambident nature of the phenoxide ion,[3] the eventual product was a C-3 para C-bonded adduct that was formed irreversibly.

Scheme I

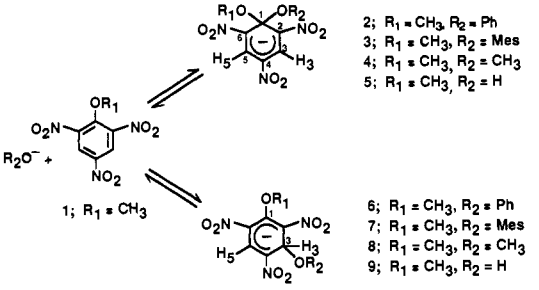

We now report that the sterically-hindered aryloxide nucleophile 2,4,6-trimethylphenoxide ion (mesitoxide, $MesO^-$), which can only react as an O-nucleophile, reacts with TNA in accord with K1T3 behavior. Thus, as with phenoxide ion, mesitoxide shows kinetic preference for C-1 attachment but differs in that the C-3 σ-adduct is thermodynamically more stable. This interesting and unexpected regioselectivity is the inverse of the standard K3T1 behavior displayed in the reaction of **1** with alkoxides and hydroxide (Scheme I).

Results and Discussion

Reaction Pathways. We have found that the reaction of 2,4,6-trinitroanisole (TNA) with mesitoxide ion in CD_3CN-glyme-d_{10} (1:1, v/v) at –40 °C gives rise to the C-1 TNA·$OMes^-$ σ-adduct **3** as the first and only detectable species by NMR spectroscopy. Figure 1a shows the 400-MHz ^1H NMR spectrum of **3** in CD_3-

® Abstract published in *Advance ACS Abstracts*, August 15, 1993.

(1) (a) Jackson, C. J.; Gazzolo, P. H. *J. Am. Chem. Soc.* **1900**, *23*, 376. (b) Meisenheimer, J. *Justus Liebigs Ann. Chem.* **1902**, *323*, 205. (c) Servis, K. *J. Am. Chem. Soc.* **1965**, *87*, 5495. (d) Servis, K. *J. Am. Chem. Soc.* **1967**, *89*, 1508. (e) Foster, R. A.; Fyfe, C. A.; Emslie, P. H.; Foreman, M. I. *Tetrahedron* **1967**, *23*, 227. (f) Bernasconi, C. F. *J. Am. Chem. Soc.* **1970**, *92*, 4682. (g) Baldini, G.; Doddi, G.; Illuminati, G.; Stegel, F. *J. Org. Chem.* **1976**, *41*, 2153. (h) Simonnin, M. P.; Pouet, M. J.; Terrier, F. *J. Org. Chem.* **1978**, *43*, 855. (i) Alaruri, A. D. A.; Crampton, M. R. *J. Chem. Res. Synop.* **1980**, 140, 2157 *J. Chem. Res., Miniprint* **1980**, and references cited therein. (j) Crampton, M. R.; Routledge, P. J.; Golding, P. *J. Chem. Soc., Perkin Trans. 2* **1981**, 526. (k) Simonnin, M. P.; Halle, J. C.; Terrier, F.; Pouet, M. J. *Can. J. Chem.* **1985**, *63*, 866.

(2) (a) Terrier, F. *Nucleophilic Aromatic Displacement*; VCH: New York, 1991. (b) Buncel, E.; Crampton, M. R.; Strauss, M. J.; Terrier, F. *Electron Deficient Aromatic- and Heteroaromatic-Base Interactions. The Chemistry of Anionic Sigma Complexes*; Elsevier: Amsterdam, 1984. (c) Terrier, F. *Chem. Rev.* **1982**, *82*, 77. (d) Artamkina, G. A.; Egorov, M. P.; Beletskaya, I. P. *Chem. Rev.* **1982**, *82*, 427. (e) Buncel, E. *The Chemistry of Functional Groups. Supplement F. The Chemistry of Amino, Nitro and Nitroso Compounds*; Patai, S., Ed.; Wiley: London, 1982. (f) Bernasconi, C. F. *MTP Int. Rev. Sci.: Org. Chem. Ser. One* **1973**, *3*, 33. (g) Strauss, M. J. *Chem. Rev.* **1970**, *70*, 667. (h) Crampton, M. R. *Adv. Phys. Org. Chem.* **1969**, *7*, 211.

(3) Buncel, E.; Dust, J. M.; Jonczyk, A.; Manderville, R. A.; Onyido, I. *J. Am. Chem. Soc.* **1992**, *114*, 5610.

0002-7863/93/1515-8985$04.00/0

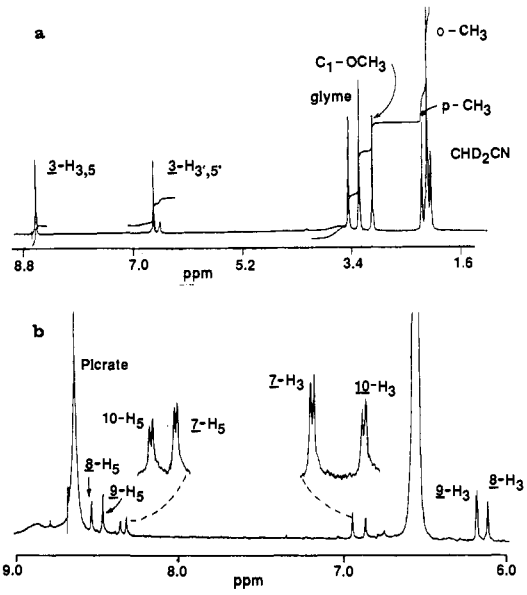

Figure 1. (a) 400-MHz ^{1}H NMR spectrum of TNA/MesOK (1:1.5), taken after 5 min of reaction time in CD_3CN–glyme-d_{10} (1:1, v/v) at –40 °C. Highlighted in the spectrum are resonances due to the C-1 TNA·OMes$^-$ adduct **3**, while some unreacted MesO$^-$ is also present. (b) 400-MHz ^{1}H NMR spectrum in the 6.0–9.0 ppm region of TNA/MesO$^-$ (1:1.5), taken after 2 h of reaction time in CD_3CN–glyme-d_{10} at 0 °C. Apparent are resonances (shown enlarged) attributed to the C-3 TNA·OMes$^-$ adduct **7** and the C-1,3 diadduct **10**. Also present are peaks due to the C-3 TNA·OMe$^-$ adduct **8**, the C-3 TNA·OH$^-$ adduct **9**, and picrate ion (**11**).

Table I. ^{1}H NMR Spectral Characteristics[a] of the Mesitoxide, Hydroxide, and Methoxide Adducts of **1** in MeCN–Glyme[b]

adduct	H-3	H-5	other
3[c]	8.62, s	8.62, s	2.93 (s, C-1 OCH_3), 6.61 (s, H-3′,5′), 2.09 (s, *p*-CH_3), 2.00 (s, *o*-CH_3)
4[d]	8.77, s	8.77, s	3.06 (s, C-1 OCH_3s)
7[e]	6.96, d, J = 1.8	8.35, d, J = 1.8	3.88 (s, C-1 OCH_3)
8[e]	6.12, d, J = 1.9	8.50, d, J = 1.9	3.82 (s, C-1 OCH_3) 3.11 (s, C-3 OCH_3)
9[e]	6.22, d, J = 1.9	8.44, d, J = 1.9	3.83 (s, C-1 OCH_3)
10[e]	6.88, d, J = 2.0	8.38, d, J = 2.0	obscured

[a] Chemical shifts are given in ppm measured at 400 MHz; coupling constants are in hertz. [b] CD_3CN–glyme-d_{10} (1:1, v/v). [c] Obtained at –40 °C. [d] Obtained at ambient temperature. [e] Obtained at 0 °C.

CN–glyme-d_{10} at –40 °C, acquired ca. 5 min after mixing the reagents (final concentrations, 0.06 M TNA and 0.09 M MesO$^-$). The NMR characteristics of **3** are as follows. ^{1}H NMR: δ 8.62 (H-3,5, s), 2.93 (C-1 OCH_3, s), 6.61 (H-3′,5′, s), 2.09 (*p*-CH_3, s), 2.00 (*o*-CH_3, s). ^{13}C NMR: δ 106.6 (C-1), 134.0 (C-2,6), 129.9 (C-3,5), 118.9 (C-4), 53.4 (C-1 OCH_3), 150.6 (C-1′), 131.7 (C-2′,6′), 129.9 (C-3′,5′), 130.5 (C-4′), 20.9 (*p*-CH_3), 18.0 (*o*-CH_3).

On subsequent monitoring of the reaction, by gradually allowing the temperature to rise above –40 °C in 5° intervals, it was found that the signals representing **3** decrease in intensity and also broaden. At –20 °C, new signals appear (in addition to those of **3**) and are ascribable to the C-3 methoxide and hydroxide adducts **8** and **9** of TNA (Table I), as previously described;[3] these products arise from solvolytic processes that generate MeO$^-$, OH$^-$, methanol, and MesOH and involve equilibration between MesOK and adventitious water in the medium. Further increase in temperature to –10 °C leads to growth in these resonances at the expense of those due to **3**.

After the solution was allowed to warm to 0 °C, new signals attributable to two different C-3 σ-adducts become clearly visible,

Scheme II

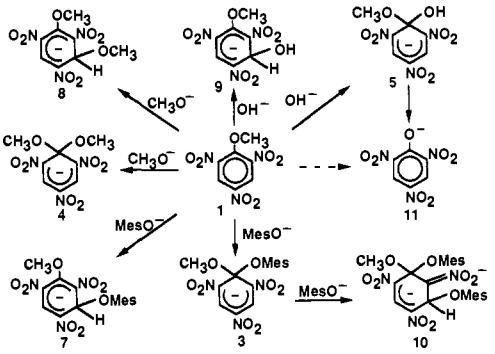

with resonances in the downfield region at δ 8.38 (H-5, d, J = 2.0), 8.35 (H-5, d, J = 1.8), 6.96 (H-3, d, J = 1.8), and 6.88 (H-3, d, J = 2.0), while upfield, a singlet at δ 3.88 is apparent, corresponding to a C-1 OCH_3 group. The downfield shift of the sp^3-attached proton, H-3 (δ 6.96 and 6.88), for these σ-adducts compared to those of corresponding protons established for **8** and **9** (ca. δ 6.20, Table I) has recently been shown by us to be consistent with bonding to the O-center of an aryloxide nucleophile.[4] Also, separate experiments showed that, like the peaks of **3**, **8**, and **9**, these new signals do not survive acidification (trifluoroacetic acid, 5 μL) as anticipated for O-adducts.[2] Thus, the signals at δ 8.35, 6.96, and 3.88 have been attributed to H-5, H-3, and the C-1 OCH_3 group, respectively, of the C-3 TNA·OMes$^-$ adduct **7**, while the resonances at δ 8.38 and 6.88 are tentatively ascribed to H-5 and H-3 of the C-1,3 diadduct **10**. In Figure 1b is shown the 6.0–9.0 ppm region of the acquired ^{1}H NMR spectrum at 0 °C; the signals attributed to the MesO$^-$ adducts **7** and **10** (shown enlarged) are clearly distinguishable from those of **8** and **9**. Above 0 °C, signals attributed to **7** and **10** disappear and peaks due to **8** and **9** also decline in favor of signals assignable to the C-1 OMe adduct **4** and the picrate ion (**11**), respectively.[3] In Table I are given the ^{1}H NMR resonances of the observed adducts, while the different reaction pathways observed in the present system are shown in Scheme II.

Our results therefore show that in the present system, MeO$^-$ and OH$^-$ conform to the standard K3T1 behavior. The C-3 adducts **8** and **9** are observed first at –20 °C, while their C-1 counterparts, **4** and picrate ion (**11**) (likely formed via **5**,[3,5] though a direct displacement route on **1** is also possible), are the final products. In contrast, the reaction of MesO$^-$ with **1** is shown to display K1T3 behavior, with formation of **3** kinetically favored, while the C-3 adduct **7** is thermodynamically more stable. These results are the first to show an O-nucleophile display kinetic preference for C-1 attachment, while the C-3 adduct is thermodynamically favored. This behavior is all the more striking because the "normal" C-3 to C-1 isomerization pathway is observed in the same system for MeO$^-$ and OH$^-$.

Stereoelectronic Factors in the C-1 σ-Complexes. Possible origins of kinetic and thermodynamic preferences in C-1 versus those in C-3 attack have been discussed by a number of workers (F-strain, charge-separated canonical forms, and geminal electronegative disubstitution, etc.).[1f-h,6] Recently,[3] we highlighted stereoelectronic factors on the basis of the analogy between acetals

(4) (a) Buncel, E.; Manderville, R. A. *J. Phys. Org. Chem.* **1993**, *6*, 71. (b) Buncel, E.; Webb, J. G. K. *J. Am. Chem. Soc.* **1973**, *95*, 8470. (c) Buncel, E.; Jonczyk, A.; Webb, J. G. K. *Can. J. Chem.* **1975**, *53*, 3761.

(5) (a) Gibson, B.; Crampton, M. R. *J. Chem. Soc., Perkin Trans. 2* **1979**, 648. (b) Bernasconi, C. F.; Fassberg, J.; Killiom, R. B., Jr.; Schuck, D. F.; Rappoport, *Z. J. Am. Chem. Soc.* **1991**, *113*, 4937.

(6) (a) Buncel, E.; Murarka, S. K.; Norris, A. R. *Can. J. Chem.* **1984**, *62*, 534. (b) Cooney, A.; Crampton, M. R. *J. Chem. Soc.*, Perkin *Trans. 2* **1984**, 1973. (c) Crampton, M. R. *J. Chem. Soc., Perkin Trans. 2* **1977**, 1442. (d) Fendler, J. H.; Hinze, W. L.; Liu, L. *J. Chem. Soc., Perkin Trans. 2* **1975**, 1768. (e) Crampton, M. R.; Gold, V. *J. Chem. Soc. B* 1966, 893. (f) Crampton, M. R.; Gold, V. *J. Chem. Soc.* **1964**, 4293.

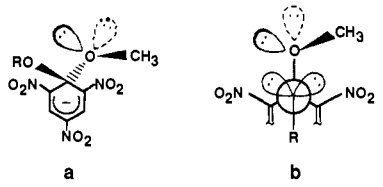

Figure 2. (a) Perspective drawing showing the antiperiplanar arrangement of the lone-pair orbital on the methoxy oxygen and the C–OR bond in C-1 σ-complexes **2** (R = Ph) and **4** (R = Me) required for stereoelectronic stabilization. (b) Newman projection diagram, viewing along the OCH_3–C-1 bond for the conformer illustrated in (a).

and C-1 dialkoxy Meisenheimer complexes.[7] Thus, as depicted in the orbital-type diagrams in Figure 2, stereoelectronic stabilization of the C-1 methoxide adduct of TNA (**4**, R = CH_3 in Figure 2) is possible through donation of lone-pair electron density from the C-1 OCH_3 oxygen to the σ^*-orbital of the C–OR bond in an antiperiplanar arrangement. This is a thermodynamic factor, and stabilization results if the C-1 σ-complexes **2**, **3**, and **4** (R = Ph, Mes, and Me in Figure 2) can achieve such antiperiplanar (lone pair to OR) conformations.

To assess the conformational preferences and the accessibility of stereoelectronic stabilization in the C-1 phenoxide and mesitoxide adducts **2** and **3** of TNA, insight can be gained through examination of the ^{13}C NMR parameters of the various adducts (Table II) and from inspection of molecular models (Darling or Fieser).

For the aryloxide σ-adducts **2** and **3**, the ^{13}C NMR chemical shifts of the ortho and para positions of the attached aryloxy moiety can be considered as reflecting the degree of orbital overlap between the p-type lone-pair orbital of the aryloxy oxygen and the aromatic π-electron system (p-π overlap) by analogy with previous studies on conformational preferences of aryl ethers.[8] When this type of overlap is operative, the ortho and para positions are shielded relative to the meta positions and the bond from the aryloxy oxygen to the substituent is approximately planar with respect to the aromatic ring. Previously,[4a] we deduced that the 1,3,5-trinitrobenzene O-adducts of phenoxide ($TNB{\cdot}OPh^-$) and mesitoxide ($TNB{\cdot}OMes^-$) prefer an approximately planar arrangement where p–π overlap is maximized. However, for **2** and **3**, inspection of Table II reveals that the ortho (C-2′,6′) and para (C-4′) positions do not resemble the corresponding shifts observed for the parent phenols and TNB adducts and downfield shifts of ca. 5.0 ppm are observed for both positions. These shifts indicate that p–π overlap is greatly diminished[8,9] and point to a conformation for **2** and **3** in which the bond from the aryloxy oxygen to the TNA^- moiety is almost perpendicular with respect to the aromatic ring.[4a,8,9]

Further scrutiny of the ^{13}C NMR parameters shows that the TNA^- chemical shift positions (C-1 → C-6) of the phenoxide adduct **2** and the methoxide adduct **4** are similar, while the shifts of the mesitoxide adduct **3** differ. The largest change in the shifts of **3** is observed for the ortho positions (C-2,6: δ 134.0) which are 4.5 ppm downfield from the corresponding positions in **2** and **4** (δ 129.5). If one works on the basis that in solution the cyclohexadienate ring of **4** is essentially planar, as indicated by X-ray structural studies,[10] then it is reasonable to assume from the analogus ^{13}C NMR parameters that the cyclohexadienate ring of the phenoxide adduct **2** is also planar. However, in the case of the mesitoxide adduct **3**, puckering of the cyclohexadienate ring may occur, as has been found by X-ray data for the $TNB{\cdot}OMe^-$ adduct.[11] In such a puckered structure for **3**, optimal stabilization of negative charge by the ortho nitro groups would be reduced because these groups are no longer coplanar with the ring, and this would result in the observed downfield shift of the ortho carbon positions.

Confirmation of the above argument follows from examination of molecular models which indicate that for **2** and **4**, stereoelectronic stabilization with the C-1 OCH_3 group antiperiplanar with respect to the C–OR bond (Figure 2) is fairly readily attainable. This conformation for **2** is depicted further in Figure 3a and shows the lack of p–π overlap referred to above. However, in the case of **3**, steric interaction between the ortho methyl groups and the ortho nitro groups in such a conformation would be quite severe. The molecular models show that puckering of the cyclohexadienate ring reduces this steric interaction but now the C-1 OCH_3 group is placed in close proximity to an ortho nitro group. To relieve this interaction, a conformation as shown in Figure 3b is adopted through rotation about the C-1–OCH_3 bond, but now the antiperiplanar arrangement of the lone pair with respect to the C-1–OMes bond is not possible. As a result, the C-1 adduct **3** becomes destabilized relative to the C-3 adduct **7**, and this then leads to the observed K1T3 behavior in which the C-3 adduct is thermodynamically more stable but formation of the C-1 adduct is kinetically preferred.

Analysis of the Energetics of C-1 and C-3 O-Adduct Formation. How Does the K3T1 Profile Slide Over to K1T3? We have previously shown that the full spectrum of regioselectivity, represented by the qualitative energy profiles shown in Figure 4, has been observed in different reaction systems.[3] Consequently, it is necessary to assess the changes in energetics that cause any given profile to metamorphose into any other. In the context of the present study pertaining to the sequence of events observed with mesitoxide as a nucleophile reacting with TNA, we now address the question: What changes in energetics cause a picryl ether–nucleophile system to become transformed from K3T1 to K1T3 (Figure 4)?[3,4a]

One can visualize three possibilities for the system to convert from the K3T1 to the K1T3 pattern of behavior. (1) If k_1^1 and k_{-1}^1 (the rate constants for formation and decomposition of the C-1 adduct, respectively) remain constant or change in such a manner that K^1 (the equilibrium constant for C-1 adduct formation) remains approximately constant, then k_1^3 (the corresponding forward rate constant for formation of the C-3 adduct) must decrease but k_{-1}^3 would have to decrease even further in order to reproduce the K1T3 pattern. (2) The inverse situation would also convert K3T1 regioselectivity into the K1T3 pattern: K^3 remains virtually constant while k_1^1 increases, but k_{-1}^1 increases even more, such that the C-1 adduct becomes thermodynamically unstable relative to the C-3 adduct. (3) Finally, a combination of an increase in k_1^1 accompanied by an even greater increase in k_{-1}^1 (smaller K^1) with a decrease in K^3 *less* than the decline in K^1 could slide the energy profile over from K3T1 to K1T3, the pattern of behavior found in the present system.

In order to obtain estimates of the energetics involved and to differentiate between the three scenarios given above, certain assumptions are necessary concerning the equivalence of the solvent media in which measurements have been made and the novel solvent system used in the present study. The majority of data in the literature concerning rates and equilibria for formation of Meisenheimer complexes has been determined in alkoxide–alcohol media or in a solvent medium of the alcohol and dimethyl sulfoxide (DMSO).[2b] However, the present study was done in

(7) (a) Kirby, A. J. *The Anomeric Effect and Related Stereoelectonic Effects at Oxygen*; Springer-Verlag: Berlin and Heidelberg, 1983. (b) Deslongchamps, P. *Stereoelectronic Effects in Organic Chemistry*; Pergamon Press: New York, 1983; pp 5–20. (c) Sinnott, M. L. *Adv. Phys. Org. Chem.* **1988**, *24*, 114.

(8) (a) Schaefer, T.; Laatikainen, R.; Wildman, T. A.; Peeling, J.; Penner, G. H.; Baleja, J.; Marat, K. *Can. J. Chem.* **1984**, *62*, 1592. (b) Buchanan, G. W.; Montaudo, G.; Finocchiaro, P. *Can. J. Chem.* **1974**, *52*, 767. (c) Dhami, K. S.; Stothers, J. B. *Can, J. Chem.* **1966**, *44*, 2855.

(9) Fujita, M.; Yamada, M. S.; Nakajima, K. I.; Nagai, M. *Chem. Pharm. Bull.* **1984**, 2622.

(10) Destro, R.; Grammicioli, C.; Simonetta, M. *Acta Crystallogr., Sect. B: Struct. Crystallogr. Cryst. Chem.* **1968**, *24*, 1369.

(11) Destro, R.; Pilati, T.; Simonetta, M. *Acta. Crystallogr., Sect. B: Struct. Crystallog. Cryst. Chem.* **1979**, *35*, 733.

Table II. ^{13}C NMR Spectral Characteristics[a] of the Phenoxide, Mesitoxide, and Methoxide C-1 Adducts of **1**, Along with Phenol and Mesitol and the 1,3,5-Trinitrobenzene (TNB) Adducts of Phenoxide ($TNB{\cdot}OPh^-$) and Mesitoxide ($TNB{\cdot}OMes^-$) in MeCN–Glyme[b]

species	C-1	C-2,6	C-3,5	C-4	C-1 OCH_3	C-1′	C-2′,6′	C-3′,5′	C-4′	*p*-CH_3	*o*-CH_3
2[c]	104.5	129.5	131.1	119.7	52.7	155.4	120.5	130.4	124.0		
3[c]	106.6	134.0	129.9	118.9	53.4	150.6	131.7	129.9	130.5	20.9	18.0
4[d]	104.5	129.5	131.1	119.2	53.2						
phenol[d]						157.5	115.4	129.5	118.9		
mesitol[d]						151.1	124.0	128.6	127.0	20.0	16.5
$TNB{\cdot}OPh^-$ [c,e]	67.9	135.1	125.8	122.6			115.0	129.0	117.3		
$TNB{\cdot}OMes^-$ [c,e]	67.8	135.1	125.8	122.6			125.0	129.8	125.0	20.8	17.3

[a] Chemical shifts are given in ppm measured at 100 MHz. [b] CD_3CN–glyme-d_{10} (1:1, v/v). [c] Obtained at –40 °C. [d] Obtained at room temperature. [e] See ref 4a.

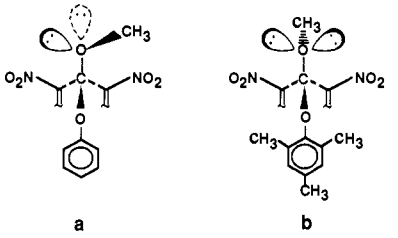

a b

Figure 3. (a) Illustration of the stereoelectronic stabilization of the C-1 phenoxide adduct **2** through antiperiplanar interaction between the lone pair on the methoxy oxygen and the C–OPh bond. (b) Illustration of the C-1 mesitoxide adduct **3**, where stereoelectronic stabilization as in (a) is not possible.

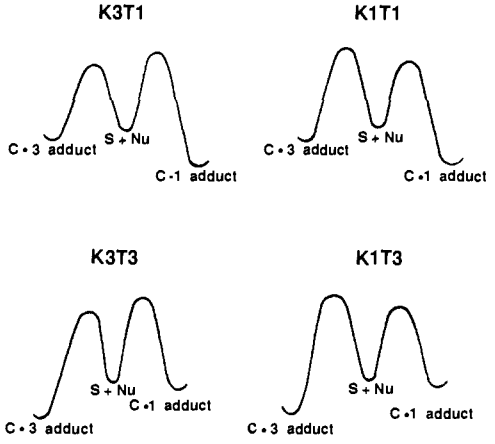

Figure 4. Qualitative energy profiles that show the four patterns of regioselectivity in Meisenheimer complex formation. K3T1 represents kinetic preference for C-3 adduct formation with thermodynamic preference for C-1 adduct formation. In K1T1, the C-1 adduct is the product of both kinetic and thermodynamic control, while in K3T3, the inverse holds. K1T3 represents kinetic preference for C-1 adduct formation with thermodynamic preference for C-3 adduct formation. Energy barriers are exaggerated for clarity. The metamorphosis from K3T1 to the K1T3 profile is discussed in detail in the text.

MeCN–glyme (50:50, v/v), which has the advantage of being fluid to temperatures as low as –50 °C. Consequently, it is important to note that while MeCN has a comparable dipole moment (μ = 3.44 D) and dielectric constant (ϵ = 37.5) to DMSO (μ = 3.9 D, ϵ = 46.48), its molecular polarizability (4.41 cm^3) is about half that of DMSO (7.99 cm^3).[12] On the other hand, glyme has a dipole moment (μ = 1.71 D) approximately half that of DMSO and a dielectric constant (ϵ = 7.20) only 15% that of DMSO,[13] but its polarizability (9.56 cm^3) is about 20% greater than that of DMSO.[14] It is not unreasonable to think, therefore, that the bulk solvent properties of a 1:1 mixture of MeCN–glyme would be similar to the solvent characteristics of DMSO or mixtures of hydroxylic solvents in the DMSO-rich region. Thus, literature values for the kinetic and equilibrium data found for adducts **4** and **8**, as well as for our model for **3**, in DMSO-rich media can be taken as a fair approximation of those that would be obtained in the present solvent system.

Bernasconi and Muller determined the Bronsted lines relating the pK_a values of phenols (para-substituted phenoxide nucleophiles) to $\log k_1^1$ and $\log k_{-1}^1$ for formation of aryloxide O-adducts of **1**.[15] Therefore, if the pK_a of mesitol in the same medium (90:10, v/v DMSO–H_2O) can be estimated, then the rate constants k_1^1 and k_{-1}^1 can be determined. In fact, extrapolation of the pK_a values for mesitol in pure H_2O and in 80 wt % DMSO–H_2O[16] yields a value of 15.16 for mesitol in the solvent used by Bernasconi and Muller. It could be argued on steric grounds that mesitol would deviate from the two Bronsted lines and that the estimated value of k_1^1 (Table III) should be viewed as an upper limit, while the predicted k_{-1}^1 value likely represents a lower limit. With these provisos, the rate constants and the equilibrium constant can be derived for **3**. Literature data[2c] for **4** and **8** were determined in MeOH-rich media and can be extrapolated similarly to the same mole fraction of DMSO used in the Bernasconi study.[15] These results are compiled in Table III.

It is immediately striking that the C-1 $TNA{\cdot}OMes^-$ adduct **3** is so unstable relative to the C-1 $TNA{\cdot}OMe^-$ adduct **4**, i.e., $\Delta\Delta G^\circ$ = 9.9 kcal·mol^{-1}, favoring **4**. In fact, **3** is also significantly less stable than the C-3 $TNA{\cdot}OMe^-$ adduct **8** ($\Delta\Delta G^\circ$ = 5.3 kcal·mol^{-1} in favor of **8**). These energetics are compatible with the fact that **3** is a transient species.

In assessing the stabilities of the adducts, it is useful to examine the free energies of activation that make up the standard free energies. In this regard, the difference in the forward activation barrier between **3** and **4** is only 0.9 kcal·mol^{-1} ($\Delta\Delta G_1^\ddagger$) for the formation of the two adducts. It is noteworthy how evenly balanced are the kinetics of these systems. The $G_1^\ddagger$ for **8** is only 1.3 kcal·mol^{-1} lower than that for **3**, while the difference in this free energy of activation for the C-3 MeO^-adduct **8** as compared to that of the C-1 MeO^- adduct **4** is only 2.2 kcal·mol^{-1}, a relatively small difference. Thus, small changes in the nucleophile can cause considerable changes in the rate and consequently the equilibrium constants and, hence, can have profound effects on the pattern of behavior of these picryl ether–nucleophile systems.

The differences in adduct stability ($\Delta\Delta G^\circ$) arise largely from differences in the ease of decomposition of the adducts back to the starting materials; for example, $\Delta\Delta G_{-1}^\ddagger$ = 10.8 kcal·mol^{-1} between **3** and **4**. The large difference in the ease of decomposition of **3** as compared to that of **4** reflects in part the difference in leaving group ability of mesitoxide as compared to that of methoxide (cf. pK_a of mesitol versus that of methanol). Note, however, that when the nucleophile is "held constant" as in the

(12) Parker, A. J. *Chem. Rev.* **1969**, *69*, 1.
(13) Riddick, J. A.; Bunger, W. B.; Sakano, T. K. *Organic Solvents. Physical Properties and Methods of Purification. Techniques of Chemistry*; Wiley: New York, 1986; Vol. II, pp 296–297.
(14) Calculated according to the equation $[(n^2-1)/(n^2+2)](M/d)(3/4N)$ given in ref 12, using data from ref 13.
(15) Bernasconi, C. F.; Muller, M. C. *J. Am. Chem. Soc.* **1978**, *100*, 5530.
(16) Baughman, E. H.; Kreevoy, M. M. *J. Phys. Chem.* **1974**, *4*, 421.

Table III. Comparison of Rate and Equilibrium Data for Adduct **3** and Adducts **4** and **8**[a]

adduct	k_1 (M^{-1} s^{-1})	k_{-1} (s^{-1})	$\Delta G_1^{\ddagger}$ [b] (kcal/mol)	$\Delta G_{-1}^{\ddagger}$ [b] (kcal/mol)	K (M^{-1})	$\Delta G°$ [c] (kcal/mol)
C-1 $MesO^-$ **3**[d]	2.6×10^4	300	11.6	14.3	87	−2.7
C-1 MeO^- **4**	4.3×10^3	2.4×10^{-6}	12.5	25.1	1.8×10^9	−12.6
C-3 MeO^- **8**	1.8×10^5	2.6×10^{-1}	10.3	18.3	7.0×10^5	−8.0

[a] Estimates for **3** refer to DMSO–H_2O 90:10, v/v at 30 °C,[15] while those for **4** and **8** were determined from data in ref 2c, extrapolated to DMSO–MeOH 80:20, v/v at 25 °C (log k versus mol fraction DMSO plots), using density data (Bicknell, R. T. M.; Davies, D. B.; Lawrence, K. G. *J. Chem. Soc., Faraday Trans. 1.* **1982**, *78*, 1595, 190, ref 13.) to make conversions from vol % to mole fraction. Both solvent systems comprise 0.696 mol fraction DMSO. [b] Calculated from the Eyring equation, cf.: Bunnett, J. F. In *Techniques in Organic Chemistry*; Weissberger, A., Ed.; Interscience: New York, 1961; Vol. VIII, Part 1, p 200, eq 11. [c] Calculated from $\Delta G° = -RT \ln K$. [d] Interpolated from the Bronsted line for substituted phenoxides reacting at C-1 of **1**, ref 15. The pK_a value for mesitol (15.16) was extrapolated to 0.696 mol fraction DMSO using the data of ref 16.

comparison of the MeO^- adducts **4** and **8**, there is also an appreciable activation free energy difference of 6.8 kcal·mol^{-1} in favor of decomposition of the C-3 adduct **8**. Although traditional steric acceleration of decomposition of **3** may also contribute to the ready decomposition of **3** relative to that of the other adducts, it is important to recognize that steric hindrance is also the root cause underlying the gradation in stereoelectronic stabilization, since suitable conformations that maximize this stabilization are sterically inaccessible to **3** and, perforce, are impossible for **8**, although readily accessible to **4**.

Although there are no numerical values available for the energetics involved in formation of the TNA·$OMes^-$ adduct **7**, it has frequently been found useful to consider a C-3 adduct of a picryl ether as being similar to a 1,3,5-trinitrobenzene adduct of the same nucleophile.[2b] In this context, we have recently unequivocally identified the $MesO^-$ adduct of TNB[4a] under the same solvent and temperature conditions used in the present work. In DMSO solvent at ambient temperature, nitro-group displacement from the TNB ring, as well as hydroxide adduct formation, apparently competes efficiently with mesitoxide adduct formation, making observation of the TNB·$OMes^-$ adduct less definitive in DMSO.[4a] It would appear, however, that since alkoxide adducts of TNB are readily observed in DMSO–ROH media at room temperature while the aryloxide adducts require low temperatures for observation, **7** as a structural analog of TNB·$OMes^-$ would also be destabilized relative to the C-3 TNA·OMe^- adduct **8**. Hence, in moving from the TNA–MeO^- system, which fits the K3T1 energy profile, to the TNA–$MesO^-$ system, which behaves according to the K1T3 energetics, both K^1 and K^3 likely decrease in magnitude but the stability of the C-1 adduct declines to a greater degree than does that of the C-3 adduct, in accord with scenario 3 outlined above. In this way, the K3T1 profile slides over to the K1T3.

In conclusion, we have shown by means of reasonable assumptions that one can derive the kinetics and thermodynamics associated with the metamorphosis of K3T1 behavior to K1T3 behavior. Moreover, a salient feature of the analysis is the significant stereoelectronic stabilization imparted to C-1 O-adducts like **4**, which if diminished, as in **3**, or clearly absent, as in **7** and **8**, results in this shift in regioselectivity. Thus, the estimation of the kinetic barriers and the thermodynamics of adduct formation lends credence to the stereoelectronic arguments that we have advanced.

Experimental Section

Materials and Methods. 2,4,6-Trinitroanisole (TNA, **1**) was prepared from picryl chloride and potassium methoxide in methanol as described previously.[17] Picryl chloride was formed from reaction of pyridinium picrate with $POCl_3$,[18] mp 83 °C. CD_3CN and glyme-d_{10} (Merck) were dried by treatment with 3A molecular sieves.[19] Potassium ethoxide solutions were prepared from freshly cut potassium metal and dry EtOH (distilled from Mg turnings) under N_2 and standardized with potassium hydrogen phthalate. 2,4,6-Trimethylphenol (mesitol, Aldrich) was recrystallized from petroleum ether. Melting points were measured on a Thomas-Hoover capillary apparatus and are not corrected.

Following the method described by Kornblum and Laurie for the preparation of potassium phenoxide,[20] potassium 2,4,6-trimethylphenoxide (MesOK) was prepared from mesitol and EtOK/EtOH as a colorless solid. Its ^1H NMR spectrum in DMSO-d_6 showed the following resonances: δ 6.38 (2H, s), 1.97 (3H, s), 1.85 (6H, s).

NMR Experiments. The NMR experiments were carried out on a Bruker AM-400 spectrometer (^1H, 400 MHz; ^{13}C, 100 MHz) in CD_3CN–glyme-d_{10} (1:1, v/v). The CD_2HCN peak (δ 1.93) served as reference and lock signal. Chemical shifts are given in parts per million (ppm) and coupling constants in hertz (Hz). For ^{13}C NMR experiments, spectra were acquired using the J-modulated (JMOD) pulse sequence.[21] Wilmad pp-507 NMR tubes (5 mm) were used in all experiments. All stock solutions and NMR tubes were capped with rubber septa and swept out with N_2 prior to injection of the reactants.

Low-Temperature NMR Experiment in MeCN–Glyme (1:1). The TNA stock solution (0.154 M) was prepared by dissolving 11.2 mg of TNA in 300 μL of CD_3CN–glyme-d_{10} (1:1, v/v), while the MesOK stock solution contained 13.0 mg of MesOK in 500 μL of solvent. Injection of 300 μL of the MesOK solution into an NMR rube and immersing the tube in liquid N_2 was followed by addition of 200 μL of TNA (final concentrations, 0.09 and 0.06 M, respectively). The contents of the tube were mixed at −50 °C (dry ice/acetone bath), and both ^1H and ^{13}C NMR parameters were recorded at −40 °C. ^1H NMR spectra of the reaction mixture were then obtained as the temperature of the system was slowly raised to ambient temperature.

Acknowledgment. This research was supported by the Natural Sciences and Engineering Research Council of Canada (NSERC). Discussions with Professors Joseph Bunnett and Julian Dust are also acknowledged.

(17) (a) Dyall, L. K. *J. Chem. Soc.* **1960**, 5160. (b) Farmer, R. C. *J. Chem. Soc.* **1959**, 3425.
(18) Boyer, R.; Spencer, E. Y.; Wright, G. F. *Can. J. Res.* **1946**, *24B*, 200.
(19) Burfield, D. R.; Smithers, R. H. *J. Org. Chem.* **1978**, *43*, 3966.
(20) Kornblum, N.; Laurie, A. P. *J. Am. Chem. Soc.* **1959**, *81*, 2705.
(21) Sanders, J. K. M.; Hunter, B. K. *Modern NMR Spectroscopy*; Oxford University Press: Oxford, 1987; pp 93–207.